The non-Abelian geometric phase in the diamond nitrogen-vacancy center

Mark A. Kowarsky,[1, 2, 3] Lloyd C. L. Hollenberg,[1, 2] and Andrew M. Martin[1]

[1] *School of Physics, The University of Melbourne, Parkville, 3010, Australia*
[2] *Center for Quantum Computation and Communication Technology, School of Physics, The University of Melbourne, Parkville, 3010, Australia*
[3] *Department of Physics, Stanford University, Stanford, CA 94305, USA*

This paper introduces a theoretical framework for understanding the accumulation of non-Abelian geometric phases in rotating nitrogen-vacancy centers in diamond. Specifically, we consider how degenerate states can be achieved and demonstrate that the resulting geometric phase for multiple paths is non-Abelian. We find that the non-Abelian nature of the phase is robust to fluctuations in the path and magnetic field. In contrast to previous studies of the accumulation of Abelian geometric phases for nitrogen-vacancy centers under rotation we find that the limiting time-scale is T_1. As such a non-Abelian geometric phase accumulation in nitrogen-vacancy centers has potential advantages for applications as gyroscopes.

PACS numbers: 03.65.Vf, 03.65.Yz, 42.50.Dv,76.30.Mi

arXiv:1402.0594v1 [quant-ph] 4 Feb 2014

Non-dynamical quantum phases are at the core of our understanding of the quantum view of the world, with historical origins going back to the work of Aharonov and Bohm[1] in 1959. In 1984 Berry developed an elegant and powerful mathematical framework[2, 3] that established the Aharonov-Bohm effect as an instance of a far more general class of phenomena[4]. This theory showed that for non-degenerate systems under an adiabatic evolution[5] of the Hamiltonian, an Abelian geometric phase is acquired[6–8]. Systems with degenerate energy levels can possess a Berry phase with a non-Abelian structure[9]. This means that different paths of the Hamiltonian produce a geometric phase that in general does not commute, allowing for richer dynamics and providing a platform to implement holonomic quantum computation[10, 11]. Recently an experiment using a superconducting circuit found unambiguous evidence[12, 13] of the non-Abelian nature of the phase[14].

The nitrogen-vacancy (NV) center in diamond offers a robust and accessible single-spin system with applications in quantum communications[15, 16], quantum information[17], nanoscale magnetometry[18–25], biosensing[26–30] and thermometry[31–33]. The NV center (for a review see Ref [34]) is a defect in diamond whereby a carbon is replaced by a nitrogen and an adjacent carbon is removed. It behaves as an electronic $^3\mathrm{A}_2$ spin triplet system in the ground state, with an excited ^{3}E state and a metastable $^1\mathrm{A}_1$ state, see Fig. 1a). A laser with a wavelength shorter than the ZPL (637 nm) polarizes the system into the $m_s = 0$ ground state and also allows the spin to be read out via the fluorescence intensity. The ground state has relatively long coherence times, even at room temperature, with the inhomogeneous broadening time $T_2^\star$ of the order of µs and the homogeneous broadening and spin relaxation times T_2 and T_1 of the order of ms[20, 35, 36]. Recently there has been work analysing the emergence of the Abelian geometric phase in the NV center in rotating systems[37–39] which could lead to using them as nanoscale gyroscopes. The ability to manipulate the magnetic sub-levels with an external magnetic field enables the possibility of degeneracy between all possible pairs of eigenstates. As such, a single NV system provides an ideal platform to study non-Abelian phases.

In this work, we show that the unique properties afforded to the NV center enable the interrogation of the non-Abelian quantum phase. It is compared with the Abelian case with limits on the angular sensitivity derived. The chief advantage of working in the non-Abelian regime is that the limiting coherence time is extended to T_1, whereas in the Abelian case the measurements are limited by T_2 or T_2^*. Such measurements would provide a platform to implement NV centers as rotational sensors that are relatively insensitive to the magnetic field noise.
.

A general non-Abelian Berry phase can be understood in terms of a Hamiltonian with N degenerate eigenstates $|a(\vec{\lambda})\rangle$, written in terms of parameters $\vec{\lambda}$ that undergo an adiabatic evolution[12]. For an initial state given by a coherent superposition of degenerate energy eigenstates, the time evolution operator is

$$U = \mathcal{P} \exp\left(- \int A_\alpha d\lambda^\alpha \right), \tag{1}$$

where $\mathcal{P}$ is the path ordering operator and α is summed over the parameters, for example $\vec{\lambda} = (\lambda^1, \lambda^2) = (\theta, \phi)$. The effective gauge potential A_α, is an $N \times N$ matrix:

$$A_{ab\alpha} = \langle a(\vec{\lambda}) | \frac{\partial}{\partial \lambda^\alpha} | b(\vec{\lambda}) \rangle, \tag{2}$$

where a and b label the degenerate eigenstates. The effect of U in general will cause a mixing between degenerate eigenstates, and unlike in the non-degenerate $U(1)$ case, the phase cannot be detected directly but only the

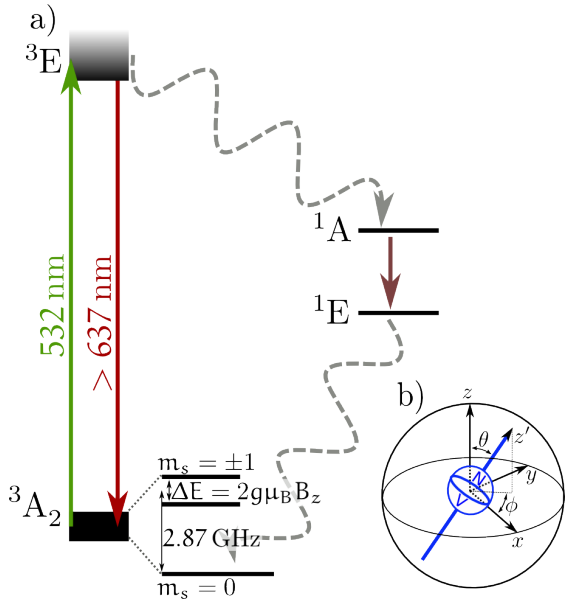

Figure 1. a) Energy level diagram of the NV center b) Geometry of the NV center. Defining the microwave pulses as the z direction, z' is the instantaneous direction of the NV axis, defined with respect to the lab frame, unprimed coordinate system, by θ and ϕ

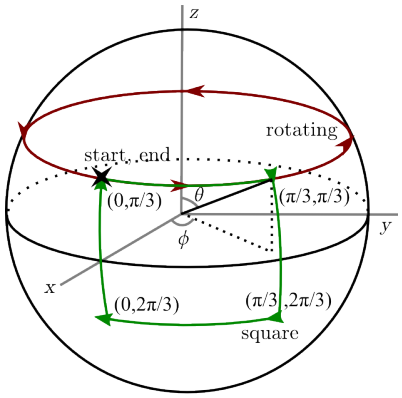

Figure 2. The two paths of rotation of the NV center considered in this paper. Both start and end in the same orientation.

trace or eigenvalues of U can be determined through a population measurement. To rigorously demonstrate the non-Abelian nature of the acquired phase, two paths in parameter space can be considered (for example those in Fig. 2, labelled 1 and 2), with equal beginning and end points. The non-Abelian nature is seen by comparing $U = U_2U_1$ with $U' = U_1U_2$. In the Abelian case $U = U'$ whereas in the non-Abelian case in general $U \neq U'$. WE now consider the specifics of the NV center.

The Hamiltonian for the NV spin triplet ground state system in the limit of a low strain diamond and with negligible hyperfine coupling is given by

$$H' = DS_{z'}^2 + \gamma \mathbf{B} \cdot \mathbf{S}, \tag{3}$$

where z' is the axis from the nitrogen atom to the adjacent vacancy, the applied magnetic field is $\mathbf{B}$, spin operator $\mathbf{S}$ and γ is the gyromagnetic ratio of the NV center, $D \approx 2.87\,\text{GHz}$ is the zero field splitting and $\hbar = 1$. In the lab frame, given by unprimed coordinates, the Hamiltonian takes the form $H = RH'R^{-1}$, where R is the rotation operator $R = \exp(-i\phi S_z)\exp(-i\theta S_y)\exp(i\phi S_z)$, where θ and ϕ map between the z and z' axes [see Fig. 1b)]. With no applied field, the $m_s = \pm 1$ states are degenerate. Applying a magnetic field along the z' axis induces a Zeeman shift of $\Delta E = \pm\gamma B_{z'}$. A normalized Hamiltonian will be considered from here on, where $H \to H/D$ and $\epsilon \equiv \gamma B_z/D$ is a measure of the separation of the energy levels. Applying a field of $\epsilon = \pm 1$ makes the $m_s = \mp 1$ and $m_s = 0$ states degenerate.

The effective gauge potential can be calculated for all pairs of states using Eq. (2). For zero applied field, the gauge potential (A is defined as $\sum_\alpha A_\alpha d\lambda^\alpha$) has the following form in the $\{|1\rangle, |-1\rangle\}$ basis

$$A = \begin{pmatrix} -i\cos\theta d\phi & 0 \\ 0 & i\cos\theta d\phi \end{pmatrix}. \tag{4}$$

This matrix is Abelian because only entries with $d\phi$ are non-zero. In fact, upon integration around a path, the diagonal entries are proportional to the solid angle enclosed and the phase is identical to the Abelian Berry phase[37, 38]. Applying a suitable magnetic field ($\epsilon = \mp 1$) along the z'-axis results in a gauge potential in the $\{|\pm 1\rangle, |0\rangle\}$ basis that has a non-Abelian nature, due to the presence of both $d\phi$ and $d\theta$ terms,

$$A = \begin{pmatrix} \mp i\cos\theta d\phi & \frac{1}{\sqrt{2}}(i\sin\theta d\phi \mp d\theta) \\ \frac{1}{\sqrt{2}}(i\sin\theta d\phi \pm d\theta) & 0 \end{pmatrix}. \tag{5}$$

To unambiguously demonstrate the non-Abelian nature of the phase at we first consider a situation when the $|0\rangle$ and $|1\rangle$ states are perfectly degenerate and the paths are exactly those as shown in Fig. 2. To maintain the degeneracy of the $|0\rangle$ and the $|1\rangle$ states, the crystal could be affixed to a magnet that supplies the constant magnetic field such that $\epsilon = -1$. The compound system could then be placed on a spinning device such that the crystal and magnet rotate together and degeneracy is maintained.

Before the whole path is considered, the mixing effect for sub-paths is examined by calculating the form of U whilst holding one of θ or ϕ constant. For $d\phi = 0$ the geometric phase in the $\{|\pm 1\rangle, |0\rangle\}$ basis is

$$\exp\left(-\int_\Theta A\right) = \begin{pmatrix} \cos(\frac{\Theta}{\sqrt{2}}) & \sin(\frac{\Theta}{\sqrt{2}}) \\ -\sin(\frac{\Theta}{\sqrt{2}}) & \cos(\frac{\Theta}{\sqrt{2}}) \end{pmatrix}, \tag{6}$$

where $\Theta = \int d\theta$ is the polar angle through which the state is rotated. This can be understood in the following manner: a physical rotation of the crystal through an

angle of Θ induces a rotation in the eigenspace of $-\Theta/\sqrt{2}$, independent of ϕ. In contrast, when $d\theta = 0$ the behaviour is dependent on θ. Setting $\theta = \pi/3$ for simplicity and rotating through an azimuthal angle Φ:

$$\exp\left(-\int_\Phi A\right) = e^{i\Phi/4}\begin{pmatrix} \cos(\frac{\sqrt{7}\Phi}{4}) + \frac{i}{\sqrt{7}}\sin(\frac{\sqrt{7}\Phi}{4}) & -i\sqrt{\frac{6}{7}}\sin(\frac{\sqrt{7}\Phi}{4}) \\ -i\sqrt{\frac{6}{7}}\sin(\frac{\sqrt{7}\Phi}{4}) & \cos(\frac{\sqrt{7}\Phi}{4}) - \frac{i}{\sqrt{7}}\sin(\frac{\sqrt{7}\Phi}{4}) \end{pmatrix}. \quad (7)$$

Expressing this in terms of the Pauli matrices, Eq. (7) can be thought of as a rotation about the axis that makes the angle $\arctan(1/\sqrt{6})$ from the negative x-axis to the z-axis. With these two segments of the paths considered, the total effect of the two paths shown in Fig. 2 can be evaluated. The first is a rotation around the sphere at $\theta = \pi/3$. The phase matrix for this is given by Eq. (7) where $\Phi = 2\pi$. The second path is a *square* in the space defined by (ϕ, θ). Each leg of the path travels along lines of constant latitude or longitude between the points given by (ϕ,θ)=$\{(0,\pi/3),\ (\pi/3,\pi/3),\ (\pi/3,2\pi/3),\ (0,2\pi/3)\}$. Over each of these sub-paths the phase accumulated has an Abelian nature, since only one of $d\phi$ or $d\theta$ are non-zero over the length of the path. The path integration can be done analytically, but its form is not concise or enlightening. A numerical approximation of it is

$$U_{\text{square}} \approx \begin{pmatrix} 0.91 + 0.23i & -0.11 - 0.33i \\ 0.34 - 0.07i & 0.66 + 0.67i \end{pmatrix}. \quad (8)$$

Since both paths start and finish at the same point, they offer the potential to show unambiguously the non-Abelian nature of the Berry phase. If the system is initially placed in the $m_s = 1$ state and traverses the two paths in one order and population of the $m_s = 1$ state is measured, then the experiment is repeated with the opposite order of the paths, the final population difference between the two paths amounts to 14.4%. This is not the optimal contrast, but demonstrates that for these paths chosen for analytical convenience, the non-Abelian effect is present.

The analysis above does not deal with experimental considerations such as decoherence, imperfect degeneracies and whether the evolution is adiabatic. Below we demonstrate that the non-Abelian phase can be measured even in non-ideal systems.

To investigate the effect of imperfect degeneracy, the Schrödinger equation ($\hbar = 1$) is written in terms of the the reduced time $s = t/T$, $i\frac{d}{ds}|\psi(s)\rangle = TH(s)|\psi(s)\rangle$, where T is the total time taken for the evolution. The general solution to this equation is $|\psi(s)\rangle = \mathcal{T}\exp\left(-iT\int H(s)ds\right)|\psi(0)\rangle$, where $\mathcal{T}$ is the time-ordering operator. Using the rotating path defined in the previous section (see Fig. 2), this was numerically solved for different values of T and of the energy separation Δ=$1+\epsilon$ for $\epsilon \approx -1$ (for $\epsilon = -1$ the $m_s = 0$ and

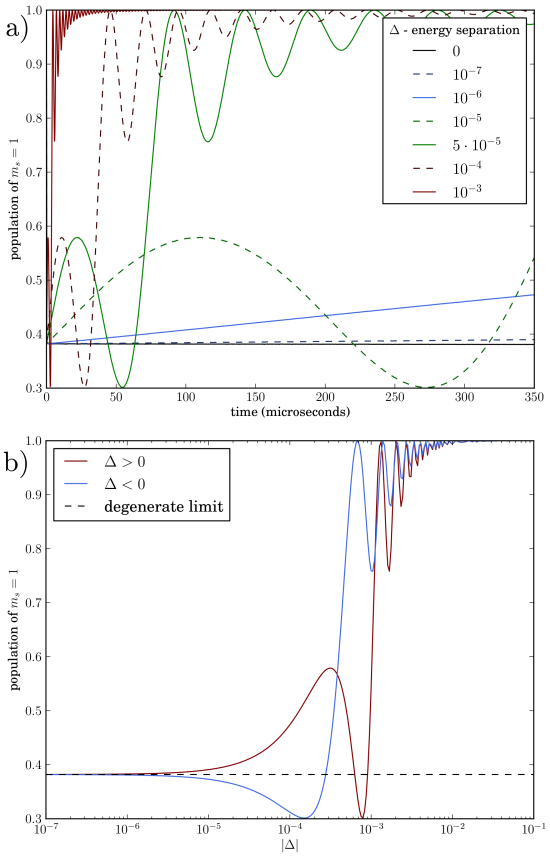

Figure 3. a) The population in the $m_s = 1$ state after evolution in the rotating path for varying degrees of degeneracy as a function of rotation time. The asymptotic degenerate result (solid black line) corresponds exactly with the expected adiabatic result. b) The effect of degeneracy for a rotation of ≈3.5 µs on the population in $m_s = 1$. Dashed line is the result expected for perfect degeneracy, which is achieved for within 5% for $|\Delta| < 2 \times 10^{-5}$.

1 states are degenerate). These calculations, for $\Phi = 2\pi$ are presented in Fig. 3a) as a function of rotation time. The maximum rotation time considered is 350 µs below (above) usual values for T_1 ($T_2^\star$) of ms (µs)[20, 35, 36] and also within potentially achievable kHz range rotational frequencies. For larger energy separations ($\Delta > 10^{-4}$) the state quickly reaches the result expected for a non-degenerate adiabatic process. As Δ is reduced, the first "dip" extends for a longer period, getting closer and closer to the result expected for true degeneracy (solid black

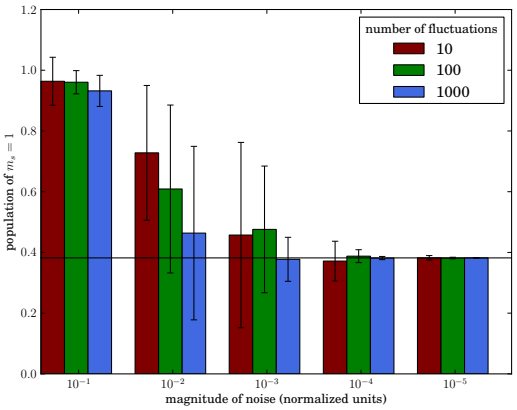

Figure 4. The effect that on-axis fluctuations, such as those due to T_2 processes has on the evolution (error bars are $\pm$ one standard deviation). For levels of noise below 1×10^{-4}, equivalent for $T = 10000$ (3.5 µs) to approximately 0.1 gauss, the effect of quickly fluctuating fields is negligible on the final system population.

line). For a fixed time, the behaviour over many orders of magnitude of degeneracy were also considered, see in Fig. 3b). For $|\Delta| < 2 \times 10^{-5}$ we find that the population of the $m_s = 1$ state is within 5% of the degenerate value [dashed line in Fig. 3)], after a complete rotation. This limit scales with evolution time and the zero-field splitting. This enforces the fact that perfect degeneracy is not required, nor are extremely long periods of evolution. All that is required is that the time of evolution is fast compared to the near degeneracy, and slow compared to the third state.

Another experimental aspect that needs to be considered is the effect that fluctuations in the magnetic field has on the evolution of the system. An ensemble of 50 NV systems was simulated in the degenerate limit, with Gaussian white noise fluctuations in the field along the NV axis for a range of magnitudes and number of events over the course of the rotating evolution. The results are summarized in Fig. 4. The primary effect of small stray fields is to break the degeneracy and induce a difference in the dynamic phase between the states considered. Since the non-Abelian experiment happens in the regime whereby the nearly degenerate states mix, this additional $U(1)$ phase does not influence the $U(2)$ evolution. This is markedly different to the Abelian experiment where fluctuations in fields increase the variance in the dynamic phase and make the geometric phase harder to recover. This is in-line with the fact that T_1, the spin relaxation time is the limit for measurements, not $T_2^\star$ or T_2 as in the Abelian experimental design.

Besides investigating the effects of a non-ideal degeneracy and non-adiabatic motion, we also considered the effects of non-ideal paths. A perfectly known path is unobtainable experimentally so in order to determine how errors in the path affect the measurement, perturbations away from the expected polar angle of $\pi/3$ were simulated for the rotating path. To remain within 5% of the expected value, the angular divergence required was found to be within 2°. In general, unlike the Abelian case which is very robust against classical fluctuations in the path[40], changes in the path have the potential to significantly affect the measurement, as different paths mix the states in non-commutative ways.

Proving the non-Abelian nature experimentally is a worthy goal, but for a single path this approach can be applied to the NV center to use it as a gyroscope. Consider a system where the $\theta = \pi/2$, from Eq. (6) after initialization and some rotation, the population remaining in the state and hence the fluorescence will be proportional to $\cos^2(\omega t/\sqrt{2})$, where ω is the frequency of rotation and t is time. For an ensemble of N centers with a collection efficiency of η and contrast of R between the $m_s = \pm 1$ and $m_s = 0$ state, the signal is given by $F = N\eta\left(1 - R\sin^2(\omega t/\sqrt{2})\right)$. The smallest detectable frequency is given by $\delta\omega = (dF/d\omega)^{-1}\delta F$, where $\delta F = \sqrt{N\eta}$ is photon shot noise. For a suitable t, $dF/d\omega = \sqrt{2}N\eta R t$ and for multiple measurements of time τ up until the limit $t = T_1$, the smallest frequency can be written as

$$\delta\omega \approx 1/\alpha R\sqrt{N\eta T_2^\star \tau}, \tag{9}$$

where $\alpha = \sqrt{2T_1/T_2^\star} > 1$ is the improvement factor over the Abelian scheme ($\alpha \equiv 1$) which is predicted to have a sensitivity of $5.4 \times 10^{-3}\,\mathrm{rad/s/Hz^{1/2}}$[38]. In general, T_1 is significantly longer than $T_2^\star$[20, 35, 36] and as such it is predicted that the sensitivity can be improved by an order of magnitude. This discussion has so far focused on the electronic spin, but it should be possible to use the ^{14}N nuclear spin in a similar fashion as it to is spin-1[37, 38, 41].

For the NV center, the required control of the Hamiltonian is carried out by rotating the diamond in physical space. With no applied magnetic field, a Ramsey pulse sequence allows the Abelian phase to be detected. Applying a magnetic field along the NV axis such that the $m_s = 0$ state is degenerate with one of $m_s = \pm 1$ allows the non-Abelian phase to be detected by reading out the population from the spin-dependent fluorescence of the center. From simulations of perturbations to the ideal motion it was found that the non-Abelian phase is robust against decohering effects from magnetic fields. An advantage of the non-Abelian experiment over the Abelian experiment is that the coherence time is increased from $T_2^\star \to T_1$ and thus the sensitivity to rotations is increased. We have shown that NV centers may be used as probes for non-Abelian geometric quantum phases, which could allow such measurements of this phase at room temperatures. Additionally, it offers the potential to be a more sensitive gyroscope though further research is needed to resolve signals from multiple axes into the 3-axis rotation.

LH and MK acknowledge support from the Australian Research Council under the Centre of Excellence scheme

(project number CE110001027). MK would like to thank D. Budker and his group for his hospitality and useful discussions relating to extensions to this work during the later stages of the manuscript's preparation.

[1] Y. Aharonov and D. Bohm, Physical Review **115**, 485 (1959).

[2] M. Berry, Proceedings of the Royal Society of London. A. Mathematical and Physical Sciences **392**, 45 (1984).

[3] B. Simon, Physical Review Letters **51**, 2167 (1983).

[4] Y. Aharonov and J. Anandan, Physical Review Letters **58**, 1593 (1987).

[5] A. Messiah, *Quantum Mechanics Volume II* (Elsevier Science B.V., 1961).

[6] J. Anandan, Nature **360**, 307 (1992).

[7] P. Leek, J. Fink, A. Blais, R. Bianchetti, M. Göppl, J. Gambetta, D. Schuster, L. Frunzio, R. Schoelkopf, and A. Wallraff, Science **318**, 1889 (2007).

[8] M. Möttönen, J. Vartiainen, and J. Pekola, Physical Review Letters **100**, 177201 (2008).

[9] F. Wilczek and A. Zee, Physical Review Letters **52**, 2111 (1984).

[10] P. Zanardi and M. Rasetti, Physics Letters A **264**, 94 (1999).

[11] J. Jones, V. Vedral, A. Ekert, G. Castagnoli, *et al.*, Nature **403**, 869 (2000).

[12] A. Zee, Physical Review A **38**, 1 (1988).

[13] X. Zhang, Z. Wang, L. Hu, Z. Zhang, and S. Zhu, New Journal of Physics **10**, 043031 (2008).

[14] A. Abdumalikov, J. Fink, K. Juliusson, M. Pechal, S. Berger, A. Wallraff, and S. Filipp, Nature (2013).

[15] T. Gaebel, I. Popa, A. Gruber, M. Domhan, F. Jelezko, and J. Wrachtrup, New Journal of Physics **6**, 98 (2004).

[16] A. Beveratos, S. Kühn, R. Brouri, T. Gacoin, J.-P. Poizat, and P. Grangier, The European Physical Journal D-Atomic, Molecular, Optical and Plasma Physics **18**, 191 (2002).

[17] T. Gaebel, M. Domhan, I. Popa, C. Wittmann, P. Neumann, F. Jelezko, J. Rabeau, N. Stavrias, A. Greentree, S. Prawer, *et al.*, Nature Physics **2**, 408 (2006).

[18] G. Balasubramanian, I. Chan, R. Kolesov, M. Al-Hmoud, J. Tisler, C. Shin, C. Kim, A. Wojcik, P. Hemmer, A. Krueger, *et al.*, Nature **455**, 648 (2008).

[19] J. Maze, P. Stanwix, J. Hodges, S. Hong, J. Taylor, P. Cappellaro, L. Jiang, M. Dutt, E. Togan, A. Zibrov, *et al.*, Nature **455**, 644 (2008).

[20] J. Taylor, P. Cappellaro, L. Childress, L. Jiang, D. Budker, P. Hemmer, A. Yacoby, R. Walsworth, and M. Lukin, Nature Physics **4**, 810 (2008).

[21] C. Degen, Applied Physics Letters **92**, 243111 (2008).

[22] J. Cole and L. Hollenberg, Nanotechnology **20**, 495401 (2009).

[23] P. Maletinsky, S. Hong, M. S. Grinolds, B. Hausmann, M. D. Lukin, R. L. Walsworth, M. Loncar, and A. Yacoby, Nature Nanotechnology **7**, 320 (2012).

[24] S. Steinert, F. Ziem, L. Hall, A. Zappe, M. Schweikert, N. Götz, A. Aird, G. Balasubramanian, L. Hollenberg, and J. Wrachtrup, Nature communications **4**, 1607 (2013).

[25] H. Mamin, M. Kim, M. Sherwood, C. Rettner, K. Ohno, D. Awschalom, and D. Rugar, Science **339**, 557 (2013).

[26] L. McGuinness, Y. Yan, A. Stacey, D. Simpson, L. Hall, D. Maclaurin, S. Prawer, P. Mulvaney, J. Wrachtrup, F. Caruso, *et al.*, Nature Nanotechnology **6**, 358 (2011).

[27] L. Hall, C. Hill, J. Cole, B. Städler, F. Caruso, P. Mulvaney, J. Wrachtrup, and L. Hollenberg, Proceedings of the National Academy of Sciences **107**, 18777 (2010).

[28] L. Hall, G. Beart, E. Thomas, D. Simpson, L. McGuinness, J. Cole, J. Manton, R. Scholten, F. Jelezko, J. Wrachtrup, *et al.*, Scientific reports **2** (2012).

[29] L. Pham, D. Le Sage, P. Stanwix, T. Yeung, D. Glenn, A. Trifonov, P. Cappellaro, P. Hemmer, M. Lukin, H. Park, *et al.*, New Journal of Physics **13**, 045021 (2011).

[30] S. Kaufmann, D. A. Simpson, L. T. Hall, V. Perunicic, P. Senn, S. Steinert, L. P. McGuinness, B. C. Johnson, T. Ohshima, F. Caruso, *et al.*, arXiv preprint arXiv:1304.3789 (2013).

[31] P. Neumann, I. Jakobi, F. Dolde, C. Burk, R. Reuter, G. Waldherr, J. Honert, T. Wolf, A. Brunner, J. H. Shim, *et al.*, Nano letters (2013).

[32] D. M. Toyli, F. Charles, D. J. Christle, V. V. Dobrovitski, and D. D. Awschalom, Proceedings of the National Academy of Sciences **110**, 8417 (2013).

[33] G. Kucsko, P. Maurer, N. Yao, M. Kubo, H. Noh, P. Lo, H. Park, and M. Lukin, Nature **500**, 54 (2013).

[34] M. W. Doherty, N. B. Manson, P. Delaney, F. Jelezko, J. Wrachtrup, and L. C. Hollenberg, Physics Reports (2013).

[35] F. Jelezko, T. Gaebel, I. Popa, A. Gruber, and J. Wrachtrup, Physical Review Letters **92**, 76401 (2004).

[36] G. Balasubramanian, P. Neumann, D. Twitchen, M. Markham, R. Kolesov, N. Mizuochi, J. Isoya, J. Achard, J. Beck, J. Tissler, *et al.*, Nature Materials **8**, 383 (2009).

[37] D. Maclaurin, M. Doherty, L. Hollenberg, and A. Martin, Physical Review Letters **108**, 240403 (2012).

[38] M. Ledbetter, K. Jensen, R. Fischer, A. Jarmola, and D. Budker, Physical Review A **86**, 052116 (2012).

[39] D. Maclaurin, L. Hall, A. Martin, and L. Hollenberg, New Journal of Physics **15**, 013041 (2013).

[40] G. De Chiara and G. Palma, Physical Review Letters **91**, 90404 (2003).

[41] R. H. Clarke, *Triplet state ODMR spectroscopy: Techniques and applications to biophysical systems* (Wiley New York, 1982).